



Tailoring propagation of light via spin-orbit interactions in correlated disorder

Federico Carlini, Nicolas Cherroret

► To cite this version:

Federico Carlini, Nicolas Cherroret. Tailoring propagation of light via spin-orbit interactions in correlated disorder. *Physical Review A*, 2022, 105 (5), pp.053508. 10.1103/PhysRevA.105.053508 . hal-03847116

HAL Id: hal-03847116

<https://hal.science/hal-03847116>

Submitted on 10 Nov 2022

HAL is a multi-disciplinary open access archive for the deposit and dissemination of scientific research documents, whether they are published or not. The documents may come from teaching and research institutions in France or abroad, or from public or private research centers.

L'archive ouverte pluridisciplinaire **HAL**, est destinée au dépôt et à la diffusion de documents scientifiques de niveau recherche, publiés ou non, émanant des établissements d'enseignement et de recherche français ou étrangers, des laboratoires publics ou privés.

Tailoring propagation of light via spin-orbit interactions in correlated disorder

Federico Carlini^{1,2} and Nicolas Cherroret¹

¹*Laboratoire Kastler Brossel, Sorbonne Université, CNRS, ENS-PSL Research University, Collège de France, 4 Place Jussieu, 75005 Paris, France*

²*MajuLab, International Joint Research Unit UMI 3654, CNRS, Université Côte d'Azur, Sorbonne Université, National University of Singapore, Nanyang Technological University, Singapore*

Based on the fundamental interplay between spatial wavefronts and polarization degrees of freedom, spin-orbit interactions (SOI) of light constitute a novel tool for optical control at the nanoscale. While well described in simple geometries, SOI of light in disordered environments, where only a partial knowledge of the material's microscopy is available, remain largely unexplored. Here, we show that in transversally random media, the disorder correlation can be exploited to tailor a variety of trajectories for ballistic beams via SOI. In particular, we unveil the existence of an oscillating spin Hall effect, stemming from the deformation of the phase of the wavefront due to SOI. In combination with a weak measurement, this phenomenon can also be maximized by an optimal choice of the disorder correlation.

Spin-orbit interactions of light refer to the interplay between the polarization and wavefront of optical beams, usually encoded in spin and orbital angular momenta. This mechanism is attracting a lot of attention as it brings about a vast number of potential applications in the control of light at the nanoscale, the optical manipulation of small objects or for metrology purposes in nanostructures (see [1, 2] for recent reviews). A particular manifestation of SOI of light is the optical spin Hall effect (SHE), an analogue of the electronic spin Hall effect that lies at the core of spintronics [3, 4]. In optics, the SHE describes transverse beam shifts occurring at a sub-wavelength scale [5]. Although naturally small, SHEs have been observed at interfaces using weak-measurement methods [6–8], in glass cylinders exploiting multiple reflection [9] or in non-paraxial configurations [10–12]. An important class of systems exhibiting SHEs are inhomogeneous materials. A seminal example are gradient-index media: while geometrical optics predicts that beam trajectories are not affected by polarization, at the wave level circularly polarized beams experience helicity-dependent transverse shifts [13, 14]. Akin to the electronic SHE where the electron spin couples to a potential gradient, in optics the photon helicity couples to the refractive-index gradient, a mechanism that can be interpreted in terms of geometric Berry phase [15, 16].

Beyond the case of a controlled inhomogeneity, it was recently shown that a SHE of light could also emerge for beams propagating in transversally disordered media [17]. In practice, clarifying the role of SOI in disordered environments is important for at least two reasons. First, because disordered materials are in general more the rule than the exception, in particular at the nanoscale where SOI typically operate. In addition, recent progresses in wave control or imaging have shown the great potential of using disorder as a tool rather than as a nuisance in general [18–23]. Whether this potential could be pushed to the realm of spin-orbit physics remains an

open question. In this Letter, we take a step in that direction by theoretically showing that the combined influence of SOI on the amplitude and the phase of the optical wavefront can be exploited to tailor a variety of transverse motions for the ballistic component of light in a disordered medium, the so-called coherent mode. This control relies on two fundamental ingredients, neglected in [17], the disorder correlation and the random variations of the refractive index. In particular, we find that a proper choice of the disorder correlation makes it possible to realize an *oscillating* SHE, see Fig. 1, and a corresponding oscillation of the beam polarization. This phenomenon, a consequence of the interferential nature of the coherent mode, was so far not known. Remarkably, while such an oscillating SHE is naturally small and may be hidden by multiple scattering, we show that these drawbacks can be both overcome. First, by a weak-measurement detection scheme allowing to amplify SOI of light to the macroscopic level and, second, by a proper tuning of the disorder correlation to minimize the propagation distance at which the SHE occurs.

Consider a monochromatic, polarized optical field $\mathbf{E}_0(\mathbf{r}_\perp) = E_0(\mathbf{r}_\perp)\mathbf{e}_0$ impinging at $z = 0$ on a three-dimensional material lying in the half-plane $z > 0$ [$\mathbf{r}_\perp = (x, y)$]. We choose $E_0(\mathbf{r}_\perp) = [2/(\pi w_0^2)]^{1/2} \exp(-r_\perp^2/w_0^2 + ik_0 x)$ with $k_0 w_0 \gg 1$, which describes a tilted, collimated beam of waist w_0 , as illustrated in Fig. 1a. The polarization vector lies in the (x', y) plane, perpendicular to the direction of propagation. We take it of the form $\mathbf{e}_0 = (\hat{\mathbf{x}}' + e^{i\phi}\hat{\mathbf{y}})/\sqrt{2}$. We focus on a dielectric medium with transverse spatial disorder: its permittivity $\epsilon(\mathbf{r}_\perp) = \bar{\epsilon} + \delta\epsilon(\mathbf{r}_\perp)$ has a random component $\delta\epsilon$ in the plane (x, y) , but is homogeneous along z [24–26]. In practice, this geometry can be realized using two-dimensional photonic lattices imprinted onto a photo-refractive crystal [24, 25] or a glass [33]. We model the disorder fluctuations by a random function of zero mean and Gaussian correlation, $\langle \delta\epsilon(\mathbf{r}_\perp)\delta\epsilon(0) \rangle = \gamma/(4\pi\sigma^2) \exp(-r_\perp^2/4\sigma^2)$, where γ is the

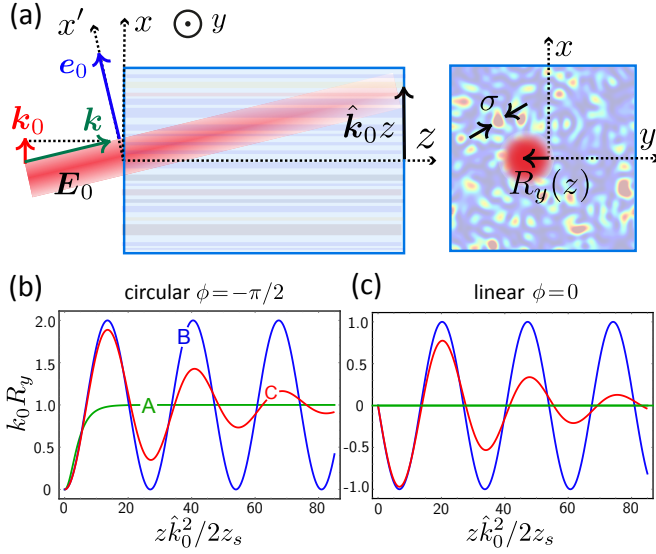


FIG. 1. (a) Propagation of a tilted beam of transverse wave vector $\mathbf{k}_0 = k_0 \hat{x}$ in a medium disordered in plane (x, y) (correlation length σ). At a distance z , the beam centroid along x is $\hat{k}_0 z$. Due to SOI, the beam also has a transverse motion $R_y(z)$ along y (spin Hall effect). (b) $R_y(z)$ for a circularly polarized incident light ($\phi = -\pi/2$), at $k_0 = 0.1$. The three trajectories correspond to the points A ($k_0\sigma = 0.62286$), B ($k_0\sigma = 0.8749$) and C ($k_0\sigma = 0.84$) in Fig. 2, where SOI respectively affect only the amplitude ($z_L = \infty$), only the phase ($z_S = \infty$) and both the phase and amplitude (z_L/z_S finite) of the wavefront. In cases B and C, a SHE oscillating around k_0^{-1} appears. (c) For a beam linearly polarized at 45° in the plane (x', y) ($\phi = 0$), a SHE is also present but oscillates around 0.

disorder amplitude, σ the correlation length and the brackets refer to disorder averaging.

As the beam propagates in the medium, the components E_j ($j = x, y, z$) of the electric field obey

$$[(\Delta + \omega^2 \epsilon(\mathbf{r}_\perp)/c_0^2) \delta_{ij} - \nabla_i \nabla_j] E_j(\mathbf{r}_\perp, z) = 0, \quad (1)$$

with ω the frequency and c_0 the vacuum speed of light. In the Letter, we study the evolution of the coherent mode, of intensity distribution is $I_c(\mathbf{r}_\perp, z) = |\langle \mathbf{E}(\mathbf{r}_\perp, z) \rangle|^2$, after a propagation distance z . The coherent mode refers to the portion of light propagating ballistically in the medium, i.e., in the forward direction \hat{x} , as opposed to light undergoing multiple scattering [27]. To access I_c , we examine the Fourier components of the average field. The latter are formally given by $\langle \mathbf{E}(\mathbf{k}_\perp, z) \rangle = \exp(ik_z z - i\Sigma z/2k_z) \tilde{\mathbf{E}}_0(\mathbf{k}_\perp)$, where $\tilde{\mathbf{E}}_0(\mathbf{k}_\perp) = \sqrt{2\pi w_0} \exp[-(\mathbf{k}_\perp - \mathbf{k}_0)^2 w_0^2/4]$ and $k_z = \sqrt{k^2 - k_\perp^2}$ with $k = \sqrt{\epsilon} \omega/c_0$ the total wavenumber. The quantity Σ , known as the self-energy tensor [27], encodes all effects of the disorder. Its real part describes how the phase of the wavefront evolves on average in the disorder (mean refractive index), while its imaginary part governs the attenuation of its amplitude (extinction

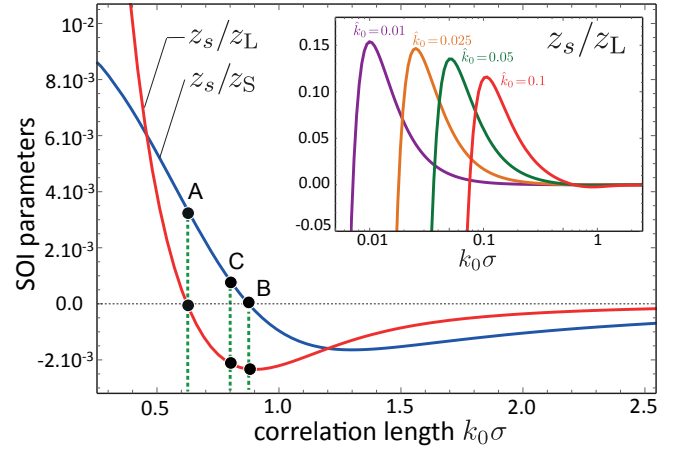


FIG. 2. Length scales z_L and z_S controlling the SHE as a function of the disorder correlation length, for $k_0 = 0.1$ and in units of the mean free path z_s . At points A and B, $z_L = \infty$ and $z_S = \infty$, respectively. At point C, both z_S and z_L are finite. The inset shows that z_S/z_L reaches a maximum at lower correlation lengths. At this maximum, the oscillating SHE occurs at the scale of a few z_s .

coefficient). An explicit calculation detailed in the Supplemental Material (SM) gives

$$\langle \tilde{\mathbf{E}}(\mathbf{k}_\perp, z) \rangle = \tilde{\mathbf{E}}_0(\mathbf{k}_\perp) e^{ik_z z} \left[e^{-i\Sigma_1 z/2k_z} \mathbf{e}_0 + \left(e^{-i\Sigma_2 z/2k_z} - e^{-i\Sigma_1 z/2k_z} \right) \mathbf{p}(\mathbf{k}_\perp) \right]. \quad (2)$$

The complex numbers Σ_1 and Σ_2 , evaluated below, are combinations of eigenvalues of Σ . The existence of two independent self-energies stems from the fact that as soon as the incident beam is tilted, i.e. $k_0 \neq 0$, the statistical isotropy in the (x, y) plane is broken, making momentum conservation along z (due to translation invariance along that direction) the unique symmetry of the problem. In Eq. (2), the first term in the right-hand side (r.h.s.) describes an evolution *without* spatial deformation. Its amplitude is controlled by Σ_1 , which defines the mean free path along z , $z_s = -k_z/\Im(\Sigma_1)$, beyond which the coherent mode is attenuated due to scattering in other directions [26, 27]. The second term in the r.h.s. is proportional to the projection $\mathbf{p}(\mathbf{k}_\perp) = (\hat{\mathbf{e}}_\perp \cdot \mathbf{e}_0) \hat{\mathbf{e}}_\perp + (\hat{\mathbf{z}} \cdot \mathbf{e}_0) \hat{\mathbf{z}}$ of the polarization onto the $(\hat{\mathbf{e}}_\perp = \mathbf{k}_\perp/k_\perp, \hat{\mathbf{z}})$ plane. It describes a wavefront deformation coupling polarization and momentum and, as such, encodes the phenomenon of spin-orbit interaction. Notice that this deformation only arises when $\Sigma_1 \neq \Sigma_2$.

To unveil the effect of the SOI term, we examine $\langle \mathbf{R}(z) \rangle = \int d\mathbf{r}_\perp \mathbf{r}_\perp I_c(\mathbf{r}_\perp, z) / \int d\mathbf{r}_\perp I_c(\mathbf{r}_\perp, z)$, the beam centroid. The first term in the r.h.s of Eq. (2) gives the main contribution to this quantity: $\langle \mathbf{R}(z) \rangle \simeq \hat{k}_0 z$. This result features a straight-line propagation with fixed polarization, see Fig. 1a. It also coincides with the prediction of the paraxial limit, where $\sim \hat{k}_0 = k_0/k \ll 1$.

Indeed, at small angle one finds $\Sigma_1 - \Sigma_2 = \mathcal{O}(\hat{k}_0^2) \rightarrow 0$, so that statistical isotropy in the (x, y) is restored and the second term in Eq. (2) vanishes. In general, however, Σ_1 and Σ_2 differ, leading to a non-trivial component $R_y(z)$ of $\langle \mathbf{R}(z) \rangle$ along the *transverse* direction y [28]:

$$R_y(z) = -\frac{\sin \phi}{k_0} \left[1 - \frac{\cos z/2z_L}{\cosh z/2z_S} \right] + \frac{\cos \phi}{k_0} \frac{\sin z/2z_L}{\cosh z/2z_S}. \quad (3)$$

This transverse motion is governed by two core parameters, $z_S = [\Im(\Sigma_2 - \Sigma_1)/k_z]^{-1}$ and $z_L = [\Re(\Sigma_2 - \Sigma_1)/k_z]^{-1}$, which represent respectively the length scales over which SOI modify the amplitude and the phase of the coherent mode. The first term in Eq. (3) was originally discovered in [17], for an elementary model of uncorrelated disordered and discarding refractive-index effects [i.e., $\Re(\Sigma_1), \Re(\Sigma_2) = 0$]. Under these approximations, $z_L \rightarrow \infty$ and $z_S \rightarrow z_s/\hat{k}_0^2$, so that $R_y(z) = -\sin \phi/k_0[1 - \cosh^{-1}(z\hat{k}_0^2/2z_s)]$. This describes a monotonic shift existing only for beams of finite helicity (or spin) $\sin \phi$. In the more realistic case considered here, however, the physics pertained to Eq. (3) is much richer since the modifications of the refractive index due to SOI give rise to spatial *oscillations* of the beam at the scale of z_L , modulating a monotonic component governed by z_S . In Eq. (2), these oscillations originate from the interference between the SOI term with itself, and between the SOI term and the paraxial one.

Both z_S and z_L are functions of \hat{k}_0 , the deviation from paraxiality, and σ , the disorder correlation. We have computed them from Σ_1 and Σ_2 , see SM. The results, shown in Fig. 2, reveal the interesting feature that z_L^{-1} and z_S^{-1} vanish at specific values of $k_0\sigma$ (points A and B, respectively). In practice, this offers the possibility to tailor various types of SHEs via σ . To illustrate this idea, we show in Fig. 1b and c the transverse motion realized for $\phi = -\pi/2$ and 0 at points A and B, as well as at point C where both z_S and z_L are finite. In configuration A, SOI only affect the amplitude of the wavefront. This leads to a monotonic increase of $R_y(z)$ toward the asymptotic value $1/k_0$ for $z \gg z_S$, effectively reproducing the result of [17]. In case B, in contrast, SOI are purely of phase origin and $R_y(z)$ exhibits oscillations around $1/k_0$. In the generic case C, finally, the oscillations are present but damped. Another interesting prediction of Eq. (3) is that an oscillating SHE can arise even for linearly polarized beams ($\phi = 0$) i.e. without initial spin, see Fig. 1c. We discuss this intriguing phenomenon below.

The SHE of the coherent mode is accompanied by an evolution of its mean polarization direction $\mathbf{e}(z)$. The latter follows from Eq. (2), using that the momentum distribution of the beam always remains peaked around \mathbf{k}_0 : $\mathbf{e}(z) \simeq \langle \tilde{\mathbf{E}}(\mathbf{k}_0, z) \rangle / |\langle \tilde{\mathbf{E}}(\mathbf{k}_0, z) \rangle|$, with

$$\langle \tilde{\mathbf{E}}(\mathbf{k}_0, z) \rangle \propto \left[e^{-i\Sigma_2 z/2k_z} \hat{\mathbf{x}}' + e^{i\phi} e^{-i\Sigma_1 z/2k_z} \hat{\mathbf{y}} \right]. \quad (4)$$

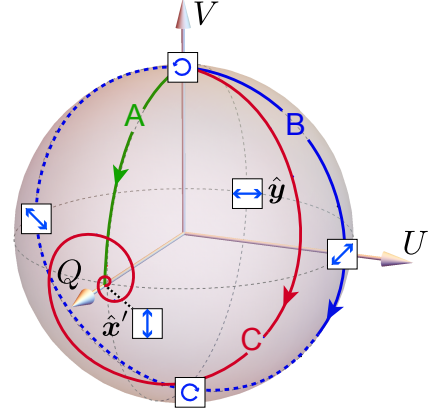


FIG. 3. Evolution of the polarization state $\mathbf{e}(z)$ on the Poincaré sphere when starting from circularly polarized beam ($\phi = \pi/2$), in configurations A, B and C. Axes are parametrized by the Stokes parameters U , V and Q .

Equation (4) showcases the breaking of statistical isotropy when $\Sigma_1 \neq \Sigma_2$. It also indicates that SOI naturally imprint *birefringence* to the random medium. From Eq. (4), we infer

$$\mathbf{e}(z) = \frac{\hat{\mathbf{x}}' + e^{i\phi + iz/2z_L} e^{-z/2z_S} \hat{\mathbf{y}}}{\sqrt{1 + e^{-z/z_S}}}, \quad (5)$$

whose evolution is represented on the Poincaré sphere of Fig. 3 for a circularly polarized beam, in the three configurations discussed above. In case A, the polarization directly turns from circular to linear following the shortest path on the Poincaré sphere. In contrast, in configuration B the oscillating SHE is associated with a permanent, periodic evolution of the helicity. In the generic case C, finally, the oscillation of helicity is damped and $\mathbf{e}(z \gg z_S)$ converges to the attractor point $\hat{\mathbf{x}}'$. Fundamentally, the dual evolutions of $R_y(z)$ and $\mathbf{e}(z)$ originate from the conservation of angular momentum

$$k_0 R_y(z) + V(z) = \text{constant} = V(0) = \sin \phi. \quad (6)$$

$V(z) = 2 \int d\mathbf{r}_\perp \Im(\langle E_x^* \rangle \langle E_y \rangle) / \int d\mathbf{r}_\perp I_c$ is the spin angular momentum (i.e., the amount of circularly polarized light in the beam, V axis in Fig. 3) and $k_0 R_y(z)$ is the beam orbital momentum, with Eq. (6) implying a mutual conversion between the two [29]. For $\phi = \pi/2$ and in case A, the initial spin is monotonically converted into orbital momentum while the beam is monotonically shifted. In cases B and C in contrast, the exchange between V and R_y involves successive mutual conversions, hence the periodic trajectories. Together with Eq. (4), the conservation of angular momentum also sheds light on the second term in Eq. (3), which predicts a SHE for a spinless incident beam, $V(0) = 0$. In that case, the beam *spontaneously* acquires a

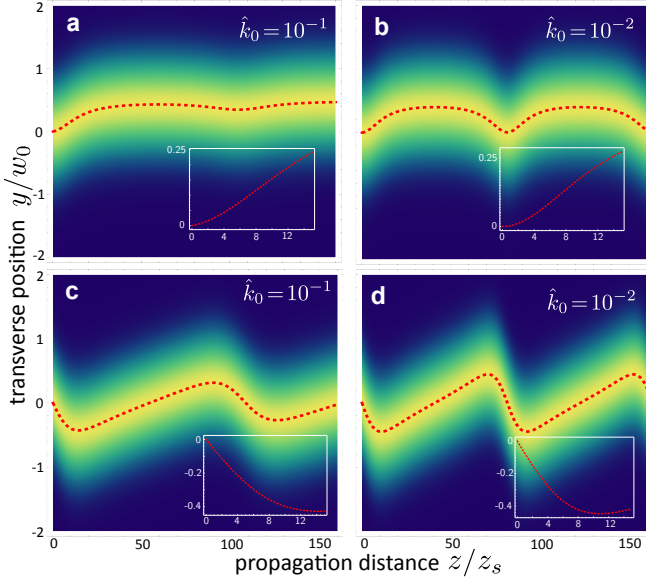


FIG. 4. Normalized intensity of the coherent mode post-selected by a polarizer \mathbf{e}_{out} (“weak measurement”): $|\langle \mathbf{e}_{\text{out}}^* \cdot \mathbf{E}(\mathbf{r}_{\perp}, z) \rangle|^2 / \int d\mathbf{r}_{\perp} |\langle \mathbf{e}_{\text{out}}^* \cdot \mathbf{E}(\mathbf{r}_{\perp}, z) \rangle|^2$. In panels a and b, $\mathbf{e}_{\text{out}} \propto \hat{\mathbf{y}} + i\delta\hat{\mathbf{x}}'$, while in panels c and d, $\mathbf{e}_{\text{out}} \propto \hat{\mathbf{y}} + \delta\hat{\mathbf{x}}'$, corresponding to an amplification of the first and second term in Eq. (3), respectively [here $k_0 w_0 = 15$ and $\delta = (k_0 w_0)^{-1}$]. Notice that the SHE is now of the order of the beam width w_0 . Dotted curves mark the centroid position $R_y(z)$. Here, $k_0 \sigma$ is chosen at the point where the ratio z_s/z_L is maximum (see inset of Fig. 2): $k_0 \sigma = 0.1056$ in panels a and c, $k_0 \sigma = 0.01005$ in panels b and d. Insets show a zoom of the $R_y(z)$ at the scale of a few z_s .

finite spin thanks to the birefringence effect, Eq. (4). A transverse motion then spontaneously appears so to satisfy Eq. (6). Interestingly, the SOI birefringence resembles the magneto-optic Voigt (or Cotton-Mouton) effect, where a magnetic field perpendicular to the direction of propagation converts a linear polarization into an elliptic one [30]. In our scenario, the role of the magnetic field is played by \mathbf{k}_0 . The analogy ends here though, since no transverse motion arises in the Voigt effect.

Under normal conditions, the oscillating SHE discovered here is tenuous for two main reasons. First, because it occurs at the scale k_0^{-1} . Although this scale greatly exceeds the optical wavelength, it remains small compared to the beam width w_0 . Second, because the coherent mode attenuates as $\exp(-z/z_s)$ due to multiple scattering. The first difficulty can be circumvented by exploiting the principle of weak quantum measurements [6, 8, 31, 32]. The idea is to start from a beam linearly polarized along $\mathbf{e}_0 = \hat{\mathbf{x}}'$. SOI then split the beam into two parts, whose far tails have finite and opposite helicities. By detecting light using a nearly-orthogonal polarizer $\mathbf{e}_{\text{out}} \propto \hat{\mathbf{y}} + i\delta\hat{\mathbf{x}}'$ with $|\delta| \ll 1$, one can then select out these tails and amplify the first term in Eq. (3) from k_0^{-1}

to w_0 . In the SM we show that a similar strategy can be used to enhance the second term in Eq. (3), using a post-selection polarizer $\mathbf{e}_{\text{out}} \propto \hat{\mathbf{y}} + \delta\hat{\mathbf{x}}'$. To overcome the attenuation of the coherent mode due to scattering, on the other hand, one can again take advantage of the disorder correlation. Indeed, as shown in the inset of Fig. 2, at a given angle $\hat{\mathbf{k}}_0$ the ratio z_s/z_L reaches a maximum at a specific σ , where z_L reduces to a few z_s . In Fig. 4, we show several types of transverse trajectories of the coherent mode computed by combining the weak measurement technique together with the maximization of z_s/z_L via σ . The insets demonstrate the possibility to realize a sizable $R_y(z)$ over distances z/z_s where the coherent mode remains observable.

We have unveiled the existence of oscillating spin Hall effects in transversally random media, controllable and amplifiable with the disorder correlation. Generally speaking, the control of SOI in disorder could be further improved using other degrees of freedom such as scatterer resonances [34] or time-dependent beams [35, 36]. Spatio-temporal SOI seem, in particular, a promising direction of research [37–39].

The authors thank D. Delande for fruitful discussions. This project has received financial support from the CNRS through the 80'Prime program, and from the Agence Nationale de la Recherche (grant ANR-19-CE30-0028-01 CONFOCAL).

-
- [1] K. Y. Bliokh, F. J. Rodríguez-Fortuño, F. Nori, and A. Zayats, *Spin-orbit interactions of light*, Nat. Photon. **9**, 796 (2015).
 - [2] F. Cardano, L. Marrucci, *Spin-orbit photonics*, Nat. Photon. **9**, 776 (2015).
 - [3] J. Wunderlich, B.-G. Park, A. C. Irvine, L. P. Zárbo, E. Rozkotová, P. Nemec, V. Novák, J. Sinova, and T. Jungwirth, *Spin Hall Effect Transistor*, Science **330**, 1801 (2010).
 - [4] D. Awschalom and M. Flatté, *Challenges for semiconductor spintronics*, Nat. Phys. **3**, 153 (2007).
 - [5] X. Ling, X. Zhou, K. Huang, Y. Liu, C.-W. Qiu, H. Luo, and S. Wen, *Recent advances in the spin Hall effect of light*, Rep. Prog. Phys. **80**, 066401 (2017).
 - [6] O. Hosten and P. Kwiat, *Observation of the spin Hall effect of light via weak measurements*, Science **319**, 787 (2008).
 - [7] Y. Qin, Y. Li, H. He, and Q. Gong, *Measurement of spin Hall effect of reflected light*, Optics Letters **34**, 2551 (2009).
 - [8] Y. Gorodetski, K. Y. Bliokh, B. Stein, C. Genet, N. Shitrit, V. Kleiner, E. Hasman, and T. W. Ebbesen, *Weak measurements of light chirality with a plasmonic slit*, Phys. Rev. Lett. **109**, 013901 (2012).
 - [9] K. Y. Bliokh, A. Niv, V. Kleiner, and E. Hasman, *Geometrodynamics of spinning light*, Nat. Photon. **2** 748 (2008).
 - [10] D. Haefner, S. Sukhov, and A. Dogariu, *Spin Hall effect of light in spherical geometry*, Phys. Rev. Lett. **102**

- 123903 (2009).
- [11] O. G. Rodríguez-Herrera, D. Lara, K. Y. Bliokh, E. A. Ostrovskaya, and C. Dainty, *Optical nanoprobeing via spin-orbit interaction of light*, Phys. Rev. Lett. **104** 253601 (2010).
 - [12] B. Roy, N. Ghosh, A. Banerjee, S. D. Gupta, and S. Roy, *Manifestations of geometric phase and enhanced spin Hall shifts in an optical trap*, New J. Phys. **16**, 083037 (2014).
 - [13] A. V. Dooghin, N. D. Kundikova, V. S. Liberman and B. Y. Zel'dovich, *Optical Magnus effect*, Phys. Rev. A **45**, 8204 (1992).
 - [14] V. S. Liberman and B. Y. Zel'dovich, *Spin-orbit interaction of a photon in an inhomogeneous medium*, Phys. Rev. A **46**, 5199 (1992).
 - [15] K. Y. Bliokh and Y. P. Bliokh *Modified geometrical optics of a smoothly inhomogeneous isotropic medium: the anisotropy, Berry phase, and the optical Magnus effect*, Phys. Rev. E **70** 026605 (2004)
 - [16] M. Onoda, S. Murakami, and N. Nagaosa, *Hall effect of light*, Phys. Rev. Lett. **93** 083901 (2004).
 - [17] T. Bardon-brun, D. Delande, and N. Cherroret, *Spin Hall Effect of Light in a Random Medium*, Phys. Rev. Lett. **123**, 043901 (2019).
 - [18] I. M. Vellekoop and A. P. Mosk, *Focusing coherent light through opaque strongly scattering media*, Opt. Lett. **32**, 2309 (2007).
 - [19] S. Popoff, G. Lerosey, M. Fink, A. C. Boccara, and S. Gigan, *Image transmission through an opaque material* Nat. Commun. **1**, 81 (2010).
 - [20] I. M. Vellekoop, A. Lagendijk, and A. P. Mosk, *Exploiting disorder for perfect focusing*, Nat. Photon. **4**, 320 (2010).
 - [21] O. Katz, E. Small, and Y. Silberberg, *Looking around corners and through thin turbid layers in real time with scattered incoherent light*, Nat Photon **6**, 549 (2012).
 - [22] O. Katz, P. Heidmann, M. Fink, and S. Gigan, *Non-invasive single-shot imaging through scattering layers and around corners via speckle correlations* Nat. Photon. **8**, 784 (2014).
 - [23] S. Rotter and S. Gigan, *Light fields in complex media: Mesoscopic scattering meets wave control*, Rev. Mod. Phys. **89**, 015005 (2017).
 - [24] T. Schwartz, G. Bartal, S. Fishman, and M. Segev, *Transport and Anderson localization in disordered two-dimensional photonic lattices*, Nature **446**, 52 (2007).
 - [25] M. Boguslawski, S. Brake, D. Leykam, A. S. Desyatnikov, and C. Denz, *Observation of transverse coherent backscattering in disordered photonic structures* Sci. Rep. **7**, 10439 (2017).
 - [26] N. Cherroret, *Coherent multiple scattering of light in (2+1) dimensions*, Phys. Rev. A **98**, 013805 (2018).
 - [27] P. Sheng, *Introduction to Wave Scattering, Localization, and Mesoscopic Phenomena*, (Academic Press, San Diego, 1995).
 - [28] Eq. (3) holds at leading order in \hat{k}_0^2 . At arbitrary value of \hat{k}_0 , the expression remains correct provided the $1/k_0$ prefactors are replaced by $(1 - \hat{k}_0^2)^{1/2}/k_0$. This implies that SOI also show up at large angle of incidence, although their amplitude tends to decrease when approaching the regime of grazing incidence.
 - [29] D. L. Andrews and M. Babiker, *The Angular Momentum of Light*, Cambridge, Cambridge University Press (2013).
 - [30] D. Budker, W. Gawlik, D. F. Kimball, S. M. Rochester, V. V. Yashchuk, and A. Weis, *Resonant nonlinear magneto-optical effects in atoms*, Rev. Mod. Phys. **74**, 1153 (2002).
 - [31] J. Dressel, M. Malik, F. M. Miatto, A. N. Jordan, and R. W. Boyd, *Colloquium: understanding quantum weak values: basics and applications*, Rev. Mod. Phys. **86** 307 (2014).
 - [32] M. R. Dennis and J. B. Götte, *The analogy between optical beam shifts and quantum weak measurements*, New J. Phys. **14**, 073013 (2012).
 - [33] M. Bellec, P. Panagiotopoulos, D. G. Papazoglou, N. K. Efremidis, A. Couairon, and S. Tzortzakakis, *Observation and optical tailoring of photonic lattice filaments*, Phys. Rev. Lett. **109**, 113905 (2012).
 - [34] A. Lagendijk and B. A. van Tiggelen, *Resonant multiple scattering of light*, Phys. Reports **270**, 143 (1996).
 - [35] M. Chalony, R. Pierrat, D. Delande, and D. Wilkowski, *Coherent flash of light emitted by a cold atomic cloud*, Phys. Rev. A **84**, 011401(R) (2011).
 - [36] C.C. Kwong, T. Yang, M. S. Pramod, K. Pandey, D. Delande, R. Pierrat, and D. Wilkowski, *Cooperative Emission of a Coherent Superflash of Light*, Phys. Rev. Lett. **113**, 223601 (2014).
 - [37] S. W. Hancock, S. Zahedpour, A. Goffin, and H. M. Milchberg, *Free-space propagation of spatiotemporal optical vortices*, Optica **6**, 1547 (2019).
 - [38] A. Chong, C. Wan, J. Chen, and Q. Zhan, *Generation of spatiotemporal optical vortices with controllable transverse orbital angular momentum*, Nat. Photon. **14**, 350 (2020).
 - [39] K. Y. Bliokh, *Spatiotemporal Vortex Pulses: Angular Momenta and Spin-Orbit Interaction*, Phys. Rev. Lett. **126**, 243601 (2021).